

Calibration of the radiation monitors from DESY and SPring-8 at the quasi-mono-energetic neutron beams using 100 and 300 MeV ${}^7\text{Li}(p,n)$ reaction at RCNP in Osaka Japan in November 2014

Albrecht Leuschner^{1,*}, Yoshihiro Asano² and Alfred Klett³

¹Deutsches Elektronen-Synchrotron, Notkestr. 85, 22607 Hamburg, Germany

²SPring-8/RIKEN, Sayo, Hyogo 679-5148, Japan

³formerly Berthold Technologies, Calmbacher Str. 22, 75323 Bad Wildbad, Germany

Abstract. At the ring cyclotron facility of the Research Center for Nuclear Physics (RCNP) Osaka University, Osaka, Japan a series of measurement campaigns had been continued with quasi mono-energetic neutron beams in November 2014. A ${}^7\text{Li}$ target was bombarded with 100 and 300 MeV protons and the generated neutron beams were directed into a long time-of-flight tunnel at 0 and 25 degrees deflection angle with respect to the proton beam. At a distance of 41 m the cross section of the neutron beam was large enough for the illumination of square meter sized objects like extended range rem-counters. The research institutes SPring-8/RIKEN, Japan, and DESY, Germany, participated in this campaign for the calibration of 4 different types of active ambient dose rate monitors: LB 6411, LB 6411-Pb, LB 6419 and LB 6420. The measurements of their responses are reported and compared with the calculated values.

1 Introduction

At the ring cyclotron facility of the Research Center for Nuclear Physics (RCNP) Osaka University, Osaka, Japan a series of measurement campaigns [1] had been continued with quasi mono-energetic neutron beams in November 2014. A ${}^7\text{Li}$ target was bombarded with 100 and 300 MeV protons and the generated neutron beams were directed into a long time-of-flight tunnel at 0 and 25 degrees deflection angle with respect to the proton beam. At a distance of 41 m the cross section of the neutron beam was large enough for the illumination of square meter sized objects like extended range rem-counters. The research institutes SPring-8/RIKEN, Japan, and DESY, Germany, participated in this campaign for the calibration of 4 different types of active ambient dose rate monitors: LB 6411, LB 6411-Pb, LB 6419 and LB 6420.

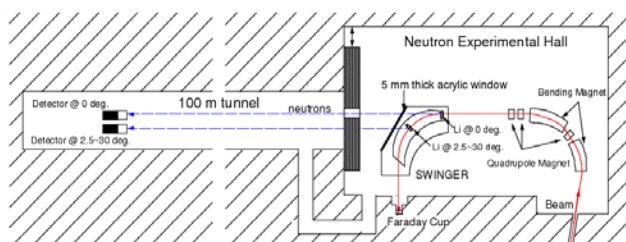


Figure 1: Geometry, proton beam: red, neutron beam: blue.

Figure 1 shows a sketch of the neutron experimental facility at RCNP. For the 25° beam conditions the Lithium target had to be moved inside the vacuum chamber of the swinger magnet and the shielding wall

(black) had to be moved to the right position as it is indicated by the arrows in figure 1. The neutron beam is characterized by time-of-flight measurements [2] and Bonner Sphere measurements [3]. The detailed characterization of the neutron beams are reported elsewhere [4]. The beam parameters are summarized in table 1. In the first column the 4 beam settings are listed.

Table 1: Neutron beam qualities for position 41 m derived from Bonner Sphere measurements [3]

Designation		Mean neutron energy [MeV]	Dose per proton charge [Sv/C]
Experimental setup	Spectral correction		
100MeV-25°		44	0.45
100MeV-0°		62	0.57
	100MeV (0.839)	98	0.20
300MeV-25°		138	0.26
300MeV-0°		205	0.39
	300MeV (0.855)	292	0.17

The second column contains the 100 MeV and 300 MeV mono-energetic neutron spectra after the spectral correction by the proposed subtraction method [1]. The mean neutron energy (3rd column) and the dose per proton charge (4th column) are derived from the dose spectrum of the Bonner Sphere measurement [3] by the inverse-square law scaling (35 m → 41 m).

* Corresponding author: Albrecht.Leuschner@desy.de

2 Method

The dose rate monitors are calibrated in terms of ambient dose equivalent $H^*(10)$. Here, it is just called dose. For the calculation of the dose response as well for the dose spectrum of the neutron beam a common set of dose conversion coefficients $H^*(10)/\Phi(E)$ [5,6] is used where Φ is the neutron fluence. It is shown in figure 2 above 0.1 MeV up to 1 GeV. $H^*(10)/\Phi(E)$ decreases from 0.1 MeV towards lower energies and is almost constant around 10 pSv cm² below 0.001 MeV down to thermal energies. This energy region is excluded as it doesn't contribute to the dose responses of the dose rate monitors from the high-energetic neutron beam.

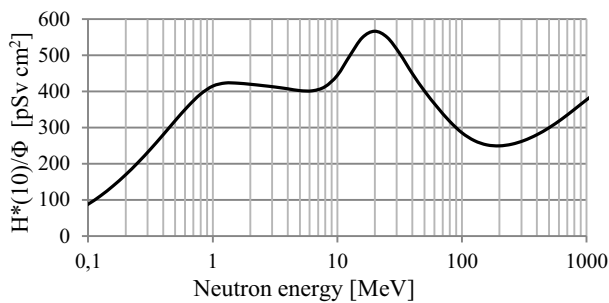


Figure 2 : Dose conversion coefficient $H^*(10)/\Phi(E)$

The dose spectra are taken from the Bonner Sphere measurements [3] using the $H^*(10)/\Phi(E)$ from above. As an example the 100 MeV spectra are shown in figure 3. The spectral correction is done with the equation

$$H(E) = H_0(E) - c \times H_{25}(E) \quad (1)$$

where $H(E)$ is the dose in the energy bin with the energy E and $H_0(E)$, $H_{25}(E)$ are the measured spectra at 0 and 25 degrees emission angle. The parameter c is obtained such that the dose integral between 0.1 MeV and 70 MeV is zero. The value of the parameter c is given in

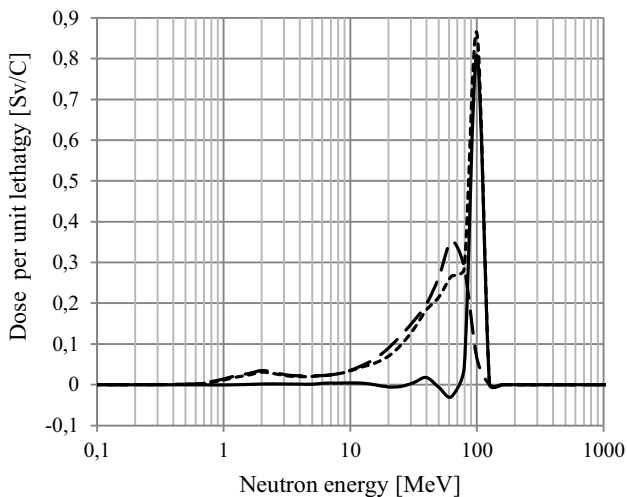


Figure 3 : Dose spectra per proton charge on target at the proton energy of 100 MeV. Angle 0° (dotted line), angle 25° (dashed line) and corrected spectrum (solid line) for position 41 m.

the 2nd column of table 1. The measured and corrected spectra are shown in figure 3 for the 100 MeV case. The corrected spectrum shows a few negative parts having no physical meaning. Nevertheless, any integrated quantity like mean energy or total dose (see table 1) are correct. The folding with a flat detector response gives a correct result. It still works well if the detector response doesn't change much within the energy range of a positive and negative wiggle. The equation (1) is applied to the dose responses of the detectors as well.

We are calling neutrons with energies below 20 MeV low-energetic neutrons and neutrons above 20 MeV high-energetic neutrons. The corresponding doses are designated H_{LEN} (low-energetic neutron dose), H_{HEN} (high-energetic neutron dose) and H_N for the entire spectrum:

$$H_N = H_{LEN} + H_{HEN} \quad (2)$$

The calculations of the detector responses were performed with the Monte-Carlo-Code FLUKA [7, 8] (FLUKA2011 versions 2b.6 and 2c.2). The devices are fully illuminated by a mono-energetic and parallel neutron beam with a rectangular cross section A . The scored quantities are given per one primary neutron. The reference dose H_{ref} at the neutron energy E is then

$$H_{ref}(E) = H^*(10)/\Phi(E) \times 1/A. \quad (3)$$

The respective response is the scored number of tritons $N(E)$ in the sensitive volume of the ³He – proportional counter for example. The response dose H_{res} is calculated by multiplying $N(E)$ with the calibration factor (H/C). For all devices N tritons are assumed to produce $C=N$ counts, i.e. the tube is 100 % efficient and the calibration factor for calculation and measurement is the same.

$$H_{res}(E) = H/C \times N(E) \quad (4)$$

3 Results on detectors

3.1 LB 6411 and LB 6411- Pb

The LB 6411 is a spherical moderated rem-counter with a ³He – proportional counter. The response R_{He} is obtained by counting the reaction products of the nuclear reaction ³He(n,p)T. The LB 6411 is designed [9, 10] to measure the low-energetic neutron dose H_{LEN} . It has been used all over the world for decades.

In order to extend the energy range the dose rate monitor LB 6411 can be equipped by an outer lead shell (10 mm Pb). The combined system is designated LB 6411-Pb [11] and measures the total neutron dose H_N . The calibrations factor is kept unchanged. In figure 4 calculated and measured responses are shown. The overresponse of the LB 6411 can be explained by contributions from the 1 MeV region of the neutron spectrum. It is the same absolute amount for the LB 6411-Pb, but due to the higher response its proportion is smaller.

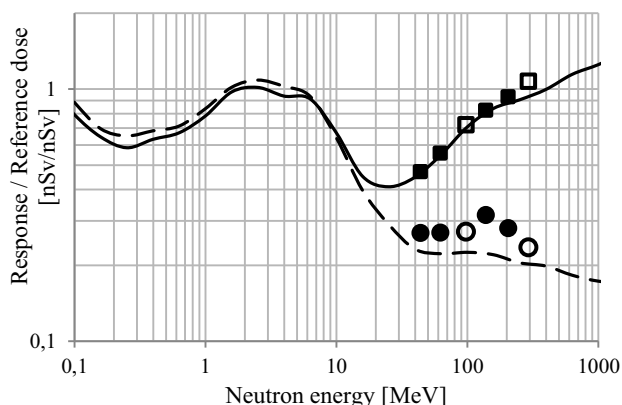


Figure 4 : Response dose divided by the reference dose of the LB 6411 (dashed, circles) and LB 6411-Pb (solid, squares); lines: calculated values; filled markers: measured values; open markers: corrected values by eq.(1).

3.2 LB 6419

The LB 6419 was designed to measure pulsed and continuous neutron and gamma radiation at high energy accelerators [12, 13]. As the proton bunch spacing of this facility is too small the capabilities for the measurement of pulsed radiation could not be tested.

The LB 6419 comprises a cylindrical moderated rem-counter with a ^3He – proportional counter and a plastic scintillator. The response of the former, R_{He} , is obtained by counting the reaction products of the nuclear reaction $^3\text{He}(n,p)\text{T}$. Its moderator is made of polyethylene and does not contain neither any response-shaping absorbers like Cd or B nor converters like Pb. So it measures H_{LEN} .

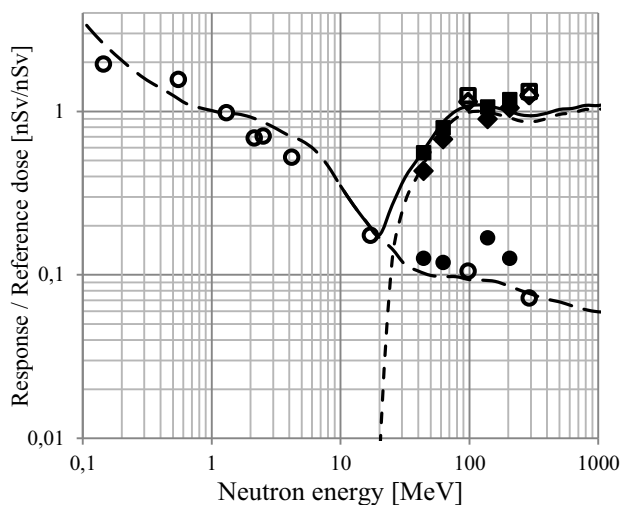


Figure 5 : Response dose divided by the reference dose of the LB 6419. Calculated response R_{He} (long dashed line) for low energy neutrons and R_{Sc} (short dashed line) for high energy neutrons. Sum of them (solid line) for the total neutron dose. Measured raw data (filled markers); measured corrected values by eq.(1) (open markers).

The response of the latter R_{Sc} is obtained by collecting scintillator light above a 20 MeV threshold.

Any responses from electro-magnetic radiation such as γ , e^\pm , μ^\pm are discriminated. The response comes from the energy deposition of charged products from neutron scattering on hydrogen nuclei of the scintillator $\text{H}(n,n)p$ and on carbon nuclei as $\text{C}(n,p)$ and $\text{C}(n,\alpha)$. It [14] measures H_{HEN} . The total neutron dose H_{N} is yielded by summing up both of the responses R_{He} and R_{Sc} .

The LB 6419 has been used at DESY since 2009. The figure 5 shows the responses of the LB 6419 detector versus the neutron energy. The response R_{He} for low energy neutrons (long dashed line) is met by the measurement (open circles) very well. Earlier measurements at the NPL [12, 15] at energies up to 20 MeV are marked with open circles. Here, low energetic stray radiation was corrected by means of shadow cones.

The measured response R_{Sc} for high energy neutrons (diamonds) comes very close to the reference value at and above 100 MeV. Its calibration was performed by measurements at CERF in 2010 and 2012 [16]. The short dashed line is a Monte Carlo calculation for the response of the scintillator. The measured sums for the total neutron dose H_{N} are marked with squares. The solid line illustrates the total neutron dose response above 10 MeV.

3.3 LB 6420

The LB 6420 is a derivative of the LB 6419 and a prototype up to now. The improvements pertain to the angular and the energy dependence of the response R_{He} by changing the shape and the structure of the moderator only. The main consequence is that the response R_{He} is assigned to the total neutron dose H_{N} here. The response R_{Sc} is for the high energy neutrons and loses its importance by becoming additional information, only.

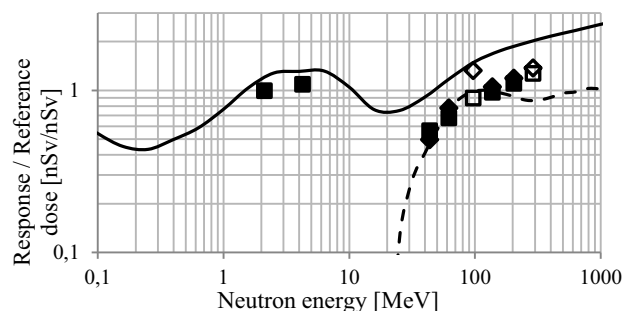


Figure 6 : Response dose divided by the reference dose of the LB 6420. Calculated response R_{He} (solid line) for all neutrons and R_{Sc} (dashed line) for high energy neutrons. Measured raw data (filled markers); measured corrected values by eq.(1) (open markers).

The figure 6 shows the responses of the LB 6420. The calibration measurements with neutron sources (^{252}Cf , $^{241}\text{AmBe}$) are marked with filled squares. The measured responses R_{He} (squares) and R_{Sc} (diamonds) fit together very well and agree with the reference. But the calculated response R_{He} for the total neutron dose is a factor of 2 too high in the 100 MeV region. This discrepancy needs further investigation.

4 Results on beam

4.1 Distance scaling on beam axis

The parameters of the neutron beams as given in table 1 were measured at 35m distance from the target. But during the measurements the detectors were located at 41 m distance. Therefore the parameters have to be scaled according to the inverse-square-law $(35 \text{ m} / 41 \text{ m})^2 = 0.72873$. This scaling factor was verified by the measurement with the LB 6419 responses for the 300 MeV, 0 degree setting. The results are given in table 2. The deviations Δ of the measured values from the inverse-square-law are on the level of a few percent.

Table 2 : Measured doses by the LB 6419 for the positions 35 m and 41 m (3rd and 4th column) compared with the inverse-square law (2nd column).

Quantity	Positions		Factor	Δ
Distance[m]	35	41	0.7287	0 %
H_{LEN} [Sv/C]	0.0719	0.0510	0.7093	-2.7 %
H_{HEN} [Sv/C]	0.539	0.397	0.7365	1.1 %

The other way round, the distance from the detector to the neutron source can be calculated by using the measured scaling factor together with the 6 m base between the positions 35 m and 41 m. The scaling factor for H_{HEN} points to the position -1 m while the scaling factor for H_{LEN} points to the position +3 m. Taking into account that 55 % of the response H_{LEN} stem from low-energetic neutrons their source is estimated to be at +6 m. The former may correspond to the target and the latter to the collimator in the shielding wall. The real geometry (see fig. 1) is very well illustrated by these data.

The different scaling for low-energetic neutrons and high-energetic neutrons leads to a small (approx. 7 %) overestimation of the low-energetic part of the Bonner Sphere dose spectrum at the position 41 m. Mostly, this effect can be neglected. But it should be considered for monitors with high response for low-energetic neutrons and low response for high-energetic neutrons like the H_{LEN} of LB 6411 and LB 6419.

4.2 Off axis neutron stray radiations

The stray radiation was measured with the LB 6419 on the tunnel floor close to the tunnel wall at the longitudinal position of approx. 44 m while the LB 6420 was in the beam at the 300 MeV, 25 degrees setting. The ratio of the stray radiation by the radiation on axis amounts to 5 % and 7 % for the high-energetic and low-energetic neutron dose, respectively.

4.3 Carbon-11 method

Since the early days of nuclear physics the Carbon-11 method has been used to measure high-energetic neutrons. It is based on the inelastic nuclear reaction

$^{12}\text{C}(n,2n)^{11}\text{C}$ in a plastic scintillator. The clean β^+ decay pattern of ^{11}C with a half-life of 20 min leads to the response from high-energetic neutrons.

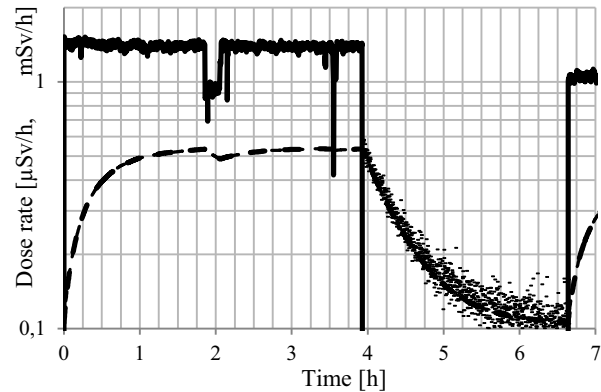


Figure 7 : History of the high-energetic neutron dose H_{HEN} of the LB 6419 (solid line) in mSv/h. The gamma dose after irradiation in $\mu\text{Sv/h}$ is marked by dots. The dashed line shows the calculated gamma dose from the ^{11}C decay in $\mu\text{Sv/h}$.

In figure 7 the history of the parasitic measurement of the high-energetic neutron dose by the C-11 method is shown. Fitting the gamma dose of the LB 6419 to the decay pattern after the irradiation (here in the period between 4 to 6.5 h) leads to a dose response from high-energetic neutrons.

The ^{11}C half-life and the dose response due to the decay of one ^{11}C nucleus are the fixed parameters while the natural background dose rate (^{40}K , cosmic muons) and the number of produced ^{11}C nuclei per H_{HEN} are fitted.

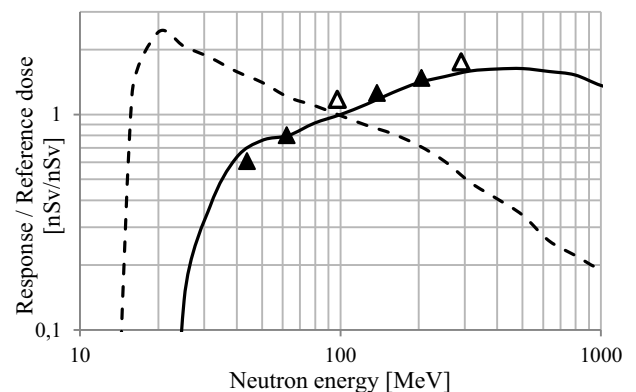


Figure 8 : High-energetic neutron dose response of the LB 6419 by means of the ^{11}C method. Solid line: FLUKA calculation for $^{12}\text{C}(n,2n)^{11}\text{C}$. Dashed line: FLUKA calculation for $^{12}\text{C}(n,p)^{12}\text{B}$. Filled triangles: measured raw data. Open triangles: measured corrected values by eq.(1).

The measurements were performed at the position 41 m in parasitic modes with the HMGU [3] and CERN [17] group, simultaneously. In figure 8 experimental results (triangles) and calculated values (solid line) are compared. They agree very well with each other. The calibration factor was chosen such that the calculated response function is correct at 100 MeV which is the typical neutron peak energy behind shieldings of high energy accelerators. Its value is set to be 5.43 nSv per ^{11}C nucleus produced in the scintillator.

Some accelerators like the electron linear accelerators FLASH, XFEL and laser plasma accelerators like LUX are operated at repetition rates of 10 Hz and lower. Here, the high-energetic neutron dose can be measured by making use of the inelastic nuclear reaction $^{12}\text{C}(n,p)^{12}\text{B}$. The ^{12}B nuclei decay with a half-life of 20 ms. Thus, there are more than 5 half-lives between successive pulses. Its response is shown in figure 8 as the dashed line. At low repetition rates the Boron-12 method can be used during exposure but the Carbon-11 cannot.

4.4 Muon and gamma contributions

The response of the LB 6419 plastic scintillator due to any electro-magnetic radiation like γ , e^\pm and μ^\pm with energies above 8 MeV contributes to the so-called muon peak at 8 MeV. This corresponds to its characteristic dimension of 4 cm. The muon peak only appears in the absorbed dose – energy spectrum in lethargy representation as shown in figure 9. The background measurement at DESY (dotted line) clearly shows the muon peak at 8 MeV. Its energy is a bit higher than that of the CERF measurement (dashed line) because of the different angular distributions of the incoming muons. The spectrum at 300 MeV, 0 degree (solid line) as well as those at the other settings do not show any hints from electro-magnetic radiation. The muon peak is missing.

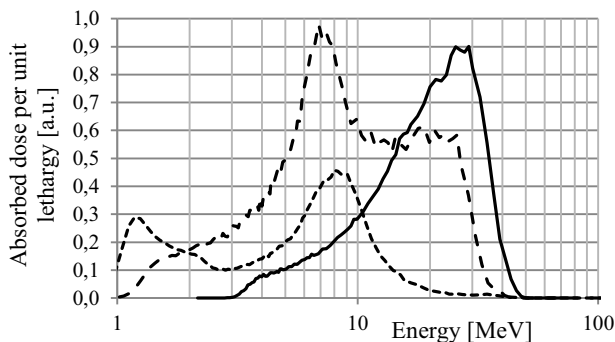


Figure 9 : Absorbed dose spectrum in lethargy representation by the plastic scintillator of the LB 6419. Solid line: RCNP, 300 MeV, 0 degree data. Dashed line: CERF, 120 GeV, CT7+2m. Dotted line: DESY, natural background.

For the experimental setup as shown in figure 1 no charged particles escape from the target chamber on the neutron beam axis as it sits in a magnetic dipole. The only candidates travelling on beam axis are photons from the π^0 decay. Another source of pions could be the neutron beam itself hitting the collimator. But again, their decay products do not appear in the spectra measured at RCNP. Their effect can be considered to be negligible.

5 Conclusions

The active neutron dose monitors LB 6411, LB 6411-Pb, LB 6419 and LB 6420 were tested in the high energy neutron beam facility at the RCNP. All the

measurements give a very consistent picture with respect to the reference doses obtained from time-of-flight and Bonner Sphere spectroscopy. The LB 6411-Pb, the LB 6419 and the LB 6420 are suited to measure high energetic neutron dose. The final results are summarized in table 3.

Table 3 : Dose responses H_N of the monitors in Sv/C proton charge on target compared to the reference BSS measurement.

Setup	BSS	LB 6411-Pb	LB 6420	LB 6419	LB 6419 C-11
100-25	0.45	0.21	0.25	0.25	0.27
100-00	0.57	0.32	0.38	0.45	0.46
100-cor	0.20	0.14	0.17	0.24	0.23
300-25	0.26	0.21	0.25	0.28	0.33
300-00	0.39	0.37	0.43	0.46	0.48
300-cor	0.17	0.18	0.22	0.23	0.30

Thanks to Prof. Tatsushi Shima, et al. from RCNP for hospitality and stable beam conditions. Thanks to Dr. Yosuke Iwamoto from JAEA and Drs. Vladimir Mares and Sebastian Trinkl from HMGU for unfolding neutron spectra and delivering reference doses. We are grateful for all the support we got from DESY, thanks to Dr. Norbert Tesch.

References

1. Yosuke Iwamoto, *Characterization of quasi-mono-energetic neutron field and radiation instruments with spectrometry using 100 and 300 MeV $^7\text{Li}(p,n)$ reaction*. Proposal for Experiment at RCNP (2013).
2. Y. Iwamoto, M. Hagiwara, D. Satoh, S. Araki, H. Yashima et al. *Characterization of high-energy quasi-mono-energetic neutron energy spectra and ambient dose equivalents of 80-389 MeV $^7\text{Li}(p,n)$ reactions using time-of-flight method*. Nucl. Instr. and Meth. A, **804**, 50–58 (2015)
3. V. Mares, S. Trinkl et al. *Neutron spectrometry and dosimetry in 100 and 300 MeV quasi-mono-energetic neutron field at RCNP, Osaka University, Japan*. This session. ICRS13, (2016)
4. Y. Iwamoto et al., *Experimental analysis of neutron and background gamma-ray energy spectra of 80-400 MeV $^7\text{Li}(p,n)$ reactions under quasi-mono-energetic neutron field at RCNP, Osaka University*. This session. ICRS13 (2016).
5. M. Pelliccioni, Overview of fluence-to-effective dose and fluence-to-ambient dose equivalent conversion coefficients for high energy radiation calculated using the FLUKA code, Radiat. Prot. Dosim. (2000); **88**:279–297.
6. International Commission on Radiological Protection (ICRP), *Conversion coefficients for use in radiological protection against external radiation*. ICRP Publication 74. Pergmon (1997).
7. T.T. Bohlen, F. Cerutti, M.P.W. Chin, A. Fassò, A. Ferrari, A. Mairani, P.R. Sala, G. Smirnov,

- V. Vlachoudis, *The FLUKA Code: Developments and Challenges for High Energy and Medical Applications*, Nuclear Data Sheets, **120**, 211-214 (2014).
8. A. Ferrari, P.R. Sala, A. Fassò, and J. Ranft, *FLUKA: a multi-particle transport code*, CERN-2005-10 (2005), INFN/TC_05/11, SLAC-R-773.
 9. A. Klett and B. Burgkhardt, *The New Remcounter LB6411: Measurement of Neutron Ambient Dose Equivalent $H^*(10)$ according to ICRP60 with High Sensitivity*, IEEE Transactions on Nuclear Science, Vol. **44**, No.3, pp. 757-759, June 1997
 10. A. Burgkhardt, G. Fieg, A. Klett, A. Plewnia, B.R.L. Siebert, *The Neutron Fluence and $H^*(10)$ Response of the New LB6411 Rem Counter*, Neutron Dosimetry, Proceedings of the Eighth Symposium, Paris, November 13-17 1995, Radiation Protection Dosimetry, Vol. **70**, Nos. 1-4, (1997), pp. 361-364.
 11. A. Klett, S. Mayer, C. Theis, H. Vincke, *A Neutron Dose Rate Monitor For High Energies*, Radiation Measurements, Elsevier, Special Issue, Volume **41**, Supplement 2, (2007) pp. 279-282
 12. A. Klett, A. Leuschner, N. Tesch, *A dose meter for pulsed neutron fields*, Radiation Measurements **45** (2010), 1242 – 1244.
 13. A. Klett, A. Leuschner, *A pulsed neutron dose monitor*, Nuclear Science Symposium Conference Record, 2007. NSS '07. IEEE, Year: 2007, Volume: **3**, 1982 – 1983.
 14. H. Dinter, B. Racky and K. Tesch, *Neutron dosimetry at high energy accelerators*, NIM A **376** (1996) 104-114.
 15. National Physical Laboratory (NPL), London, UK, <http://www.npl.co.uk/science-technology/neutron-metrology/products-and-services/monoenergetic-neutron-fluence-and-dose-standards>
 16. CERF-EU, Genf, <http://cerf-dev.web.cern.ch/>
 17. R. Garcia Alia et al. *SEE cross section calibration and application to quasi-mono-energetic and spallation facilities*. This session. ICRS13, (2016)